doi:10.1006/jmbi.2000.4501 available online at http://www.idealibrary.com on IDEAL® J. Mol. Biol. (2000) 302, 873–885

JMB

Viral Escape at the Molecular Level Explained by Quantitative T-cell Receptor/Peptide/MHC Interactions and the Crystal Structure of a Peptide/MHC Complex

Alain C. Tissot, Carlo Ciatto, Peer R. E. Mittl, Markus G. Grütter and Andreas Plückthun*

Biochemisches Institut der Universität Zürich Winterthurerstrasse 190 CH-8057, Zürich Switzerland

*Corresponding author

Viral escape, first characterized for the lymphocytic choriomeningitis virus (LCMV) in a mouse transgenic for the P14 T cell-receptor (TCR), can be due to mutations in T-cell epitopes. We have measured the affinity between the H-2D^b containing the wild-type and two of its ''viral escape'' epitopes, as well as other altered peptide ligands (APL), by using BIACORE analysis, and solved the crystal structure of H-2D^b in complex with the wild-type peptide at 2.75 Å resolution. We show that viral escape is due to a 50 to 100-fold reduction in the level of affinity between the P14 TCR and the binary complexes of the MHC molecule with the different peptides. Structurally, one of the mutations alters a TCR contact residue, while the effect of the other on the binding of the TCR must be indirect through structural rearrangements. The former is a null ligand, while the latter still leads to some central tolerance. This work defines the structural and energetic threshold for viral escape.

Keywords: alpha-beta T-cell receptors; major histocompatibility complex; viral escape; receptor ligand interaction; crystal structure

Introduction

Viruses have developed several mechanisms to escape the immune response of their hosts (reviewed by Zinkernagel, 1996; Borrow & Shaw, 1998; McMichael, 1998). One of these mechanisms was first revealed in studies on virus mutants, which were no longer cleared in a mouse transgenic for the P14 T-cell receptor (TCR) infected with the lymphocytic choriomeningitis virus (LCMV), in contrast to the wild-type (wt) mouse (Pircher *et al*., 1990). These viruses had acquired mutations in T-cell epitopes of the glycoprotein, which abolished recognition by the transgenic cytotoxic T-lymphocytes (CTL). Therefore, the mutation rate of the RNA virus was high enough and the selective pressure created in the transgenic T-cell situation was strong enough such that variants escaping the immune response could emerge. The same mechanism of escape from CTL control has been demonstrated in other viral infections such as HIV and hepatitis B virus (Bertoletti *et al*., 1994; Klenerman *et al*., 1994). It is interesting that some of these epitopes behaved as antagonists even at substoichiometric ratios relative to the wt epitope (Bertoletti *et al*., 1994; Klenerman *et al*., 1994), while other escape epitopes needed to be present in excess over the wt ligand (Klenerman *et al*., 1994; Sewell *et al*., 1997).

Variant T-cell epitopes, known as altered peptide ligands (APL), have been identified which elicit only part of the spectrum of T-cell responses, or can even antagonize the response to an agonist epitope when presented on the same target cell (reviewed by Sloan-Lancaster & Allen, 1996). They are identified by differences in the pattern of phosphorylation of ZAP-70 and TCR-associated ζ-chains (Germain & Stefanova, 1999). APL epitopes have been isolated both for CD4 and CD8 T-cells (Sloan-Lancaster & Allen, 1996). Current models favor a discrimination between agonists, weak agonists, partial agonists and antagonists, based on the life-time of the interaction, i.e. the off-rate (Davis *et al*., 1998; Ding *et al*., 1999; Germain & Stefanova, 1999).

Abbreviations used: APL, altered peptide ligand; CTL, cytotoxic T-lymphocyte; LCMV, lymphocytic choriomeningitis virus; pMHC, peptide-MHC complex; TCR, T-cell receptor; wt, wild-type; RU, resonance units.

E-mail address of the corresponding author: plueckthun@biocfebs.unizh.ch

0022-2836/00/040873–13 $35.00/0

Several structures of TCRs alone or bound to peptide-MHC complexes (pMHC) have now been solved (reviewed by Garcia *et al*., 1999; Reinherz *et al*., 1999), and provide a basis for understanding the structural basis of cross-reactivity. In particular, Wiley and co-workers have solved crystal structures of four complexes between the same TCR and pMHC complexes harboring either a strong agonist, a weak agonist, or two different weak antagonists (Garboczi *et al*., 1996; Ding *et al*., 1999). The comparison of the structures revealed that cross-reactivity between the ligands was achieved by small structural rearrangements in the peptide, the MHC and the TCR (Ding *et al*., 1999). The extent of structural rearrangements, however, did not correlate with the differences in intracellular signaling events (Ding *et al*., 1999) or the classification of the peptides as weak agonists or antagonists. The changes induced on the pMHC surface upon going from the wt to an antagonist epitope have also been studied crystallographically by McMichael and coworkers (Reid *et al*., 1996). They found essentially three types of structural changes in the pMHC complex: a mere movement of the side-chains exposed to the TCR, conformational changes in the peptidic backbone, and conformational changes in both the peptide and the MHC molecule.

We have investigated here the binding of the recombinant P14 TCR to pMHCs carrying viral epitopes originally isolated in the transgenic mouse model described above, infected with the LCMV virus. Four variants of the immunodominant gp33 epitope, KAVYNFATC, leading to viral escape were described (Pircher *et al*., 1990), and we studied the two best characterized ones. These are the peptides V3L (Val3 to Ala), and Y4F (Tyr4 to Phe), respectively.

Here, we have also solved the crystal structure of H-2D^b with the wt ligand, which gives a structural basis for understanding the binding of the various peptides to the MHC molecule and to model the effect on TCR recognition. We also extended our study to other APLs, thereby covering the whole range of peptide variants from full agonists to weak agonists and finally to antagonist peptides. Our measurements allow us therefore to rank the affinity of pMHC carrying viral escape epitopes isolated *in vivo* within the range of affinities obtained for APLs identified *in vitro* and to directly correlate these measurements with current models of T-cell activation. This is, to our knowledge, the first characterization of the affinities of the TCR for pMHC containing viral escape epitopes.

Results

Expression and purification of MHC and TCR

The pMHC complexes were obtained by expressing the individual subunits in *Escherichia coli*, and were refolded together with the peptide. They were then purified as described by Tissot *et al*. (2000). The TCR was refolded and purified from the α and β-chain expressed individually as inclusion bodies in *E. coli*, and purified by gel filtration as described (Tissot *et al*., 2000).

The pMHC complexes were isolated by gel filtration for all peptides investigated, confirming that these bind H-2D^b, and that the pMHC complexes are stable. This is in agreement with measurements of MHC stabilization by the peptides on RMA-S cells, as determined for the wt as well as the A4Y and F6YT8S epitopes (Bachmann *et al*., 1996; Sebzda *et al*., 1996). The original gp33 protein sequence contains Cys at position 41, but most experiments with isolated peptides were carried out with peptides containing Met at this position, for reasons of stability against air oxidation. We also used the Met peptide in this study (Pircher *et al*., 1993; Bachmann *et al*., 1996; Sebzda *et al*., 1996). To distinguish the two, we call the Met-containing peptide gp33, and the Cys-containing one gp33c. We solved the crystal structure of the Cys-containing epitope (gp33c). As demonstrated below from a comparison of our structure with the structure of H-2D^b in complex with the np366 peptide from the influenza virus (Young *et al*., 1994), which contains Met in position P9, both peptides can be used interchangeably. For the V3L and Y4F peptides, binding to the MHC was independently demonstrated in an indirect way in cytotoxic assays, where target cells pulsed with the peptides were killed by CTLs raised against LCMV from C57BL/6 mice (Pircher *et al*., 1990), showing that the peptides must have been presented by H-2D^b.

SPR measurement

The affinity between the P14 TCR and the various pMHCs, containing the wt or APLs, was determined by BIACORE measurements. The TCR was non-covalently bound to the sensor chip surface, using an anti-Cβ monoclonal antibody, in turn covalently derivatized to the chip (Tissot *et al*., 2000). This is equivalent to an affinity chromatography step, as misfolded and aggregated TCR does not seem to bind, and has the advantage of avoiding loss of activity during regeneration, since new TCR is injected for each measurement. The dissociation of the TCR from the anti-Cβ monoclonal antibody is so slow that it is negligible during the plateau phase of pMHC binding. Roughly 4000 RUs of monoclonal antibody were derivatized on the surface. The TCR was injected at a concentration of 0.8 or 1.6 μM, which resulted in the binding of approximately 700 to 1000 RUs. Within each experiment, the variation of the level of TCR bound to the chip at each injection was within 10 % of the average, and appeared to be random, not showing any systematic trend. As described by Tissot *et al*. (2000), the binding of the gp33-pMHC to the P14 TCR, in turn bound to the anti-Cβ monoclonal antibody on the chip, is specific, since

other H-2D^b complexes containing non-cognate peptides do not bind to the same surface at the same concentration.

The determination of each dissociation constant was performed using the same TCR concentration for immobilization on the anti-Cβ monoclonal antibody for all measurements. The pMHCs were then injected on this surface at different concentrations, and as described by Tissot *et al*. (2000), the binding of the pMHC to the immobilized TCR rapidly reached equilibrium, which is reflected in the plateau shape of the curve. The pMHCs were also injected on an inactivated blank surface as a reference as described by Tissot *et al*. (2000). The signal on the reference surface was subtracted from the signal obtained on the TCR surface, to give the corrected signal, which was used to obtain the dissociation constant (K_D). Both the TCR and the reference surface were regenerated after each injection, and fresh TCR was injected for each measurement. Binding of the pMHCs to the anti-Cβ monoclonal antibody alone was checked by injecting pMHC over the anti-Cβ surface devoid of TCR, and no binding was observed.

The kinetics of the pMHCs injected over the TCR surface and the reference surface was both too fast and at the limit of the instrumental mixing time (Tissot *et al*., 2000). Therefore, the dissociation phases of the pMHC injected on either the TCR or reference surface could not be fitted reliably. Increasing the flow rate to 30 μl/min did not affect the difference between the dissociation phases on TCR and reference surface, respectively, indicating that the dissociation phase cannot be obtained with confidence. Weak interactions between the pMHC and the sensorchip surface lead to a discernable tail (Figure 1(a)), while BSA injected at the same flow-rate on the TCR surface displayed an almost perfect ''square wave'' form of the kinetics and therefore a much faster kinetics than the pMHC on either the TCR or reference surface. We therefore used the plateau levels for the reliable K_D determination for the pMHC/TCR complexes.

Viral escape epitopes

We first investigated the binding of the two variant peptides which were isolated from viruses found to escape the immune response of the host in the transgenic P14 TCR mouse model. These are the Y4F and V3L epitopes. The V3L epitope shows weak binding, which can still be fitted to a hyperbolic curve (Figure 1(b), Table 1). This results in a saturation binding value of 466 RUs, in agreement, within experimental error, with the value of 550 RUs obtained for the wt epitope on the same surface using the same batch of TCR. The Y4F-pMHC did not show saturation of the signal within the concentration range measured (Figure 1(b)), reflecting a very weak binding, and prohibiting any K_D determination. In order to obtain an approximation for its K_D value, we performed a fit to a hyperbolic binding curve in which we fixed the value of RU_{max} to the average RU_{max} value (467 RUs) obtained with the wt, F6YT8S, V3L and Y4A-epitopes containing pMHCs, injected on the same surface and using the same batch of TCR (Table 1). This yielded a K_D value of approximately 680 μM. Changing the value of RU_{max} to the value obtained with the wt-pMHC (550 RUs) raised the K_D value to 800 μM, illustrating the range of error inherent to the procedure, but also that the order of magnitude is quite robustly determined. The affinities of the pMHCs containing both the V3L and Y4F epitopes are therefore 50, and 100-fold lower, respectively, than the affinity of the P14 TCR for the wt gp33-pMHC (Table 1).

Table 1. Effects of epitope variants on T-cell ativity and K_D

Peptide	Lysis	Proliferation	Virus clearance	Central tolerance	K_D (μM)[a]
KAVYNFATM (wt)	+	+	+	+	6(± 0.2)
KAVYNYASM (F6Y/T8S)[b]	+	+	n.d.	n.d.	15(± 0.9)
KAVANFATM (Y4A)[c]	+/−	+/−	n.d.	n.d.	35(± 7.7)
KALYNFATM (V3L)[d]	−	−	−	+/−	264(± 103)
KAVFNFATM (Y4F)[d]	−	n.d.	−	n.d.	681
KAVSNFATM (Y4S)[c,e]	n.d	n.d	n.d	n.d	530

The effects of substitutions in the gp33 epitope on the dissociation constant K_D and on T-cell activation as measured by cytotoxicity, proliferation, virus clearance and central tolerance. Lysis refers to the ability of the target cell loaded with the corresponding peptide to elicit cytotoxicity when brought in contact with the P14 T-cell clone. Proliferation refers to the ability of the P14 T-cell clone to proliferate when brought in contact with target cells loaded with the corresponding peptide. Virus clearance refers to clearance of the LCMV virus bearing either the wt or mutated glycoprotein containing the mutations of the corresponding peptide in mice infected with the virus. Central tolerance indicates the ability of the LCMV virus bearing the glycoprotein containing either the wt or mutant epitope to induce deletion of the transgenic T-cells in neonatally infected mice. K_D is the dissociation constant calculated as described in Materials and Methods and Results. n.d., not determined.

[a] Determined by BIACORE analysis.
[b] Bachmann *et al*. (1996).
[c] Sebzda *et al*. (1996).
[d] Pircher *et al*. (1990).
[e] Antagonist peptide. An alternative way of fitting the data could yield a lower K_D value, with binding only to a fraction of the molecules (see Results).

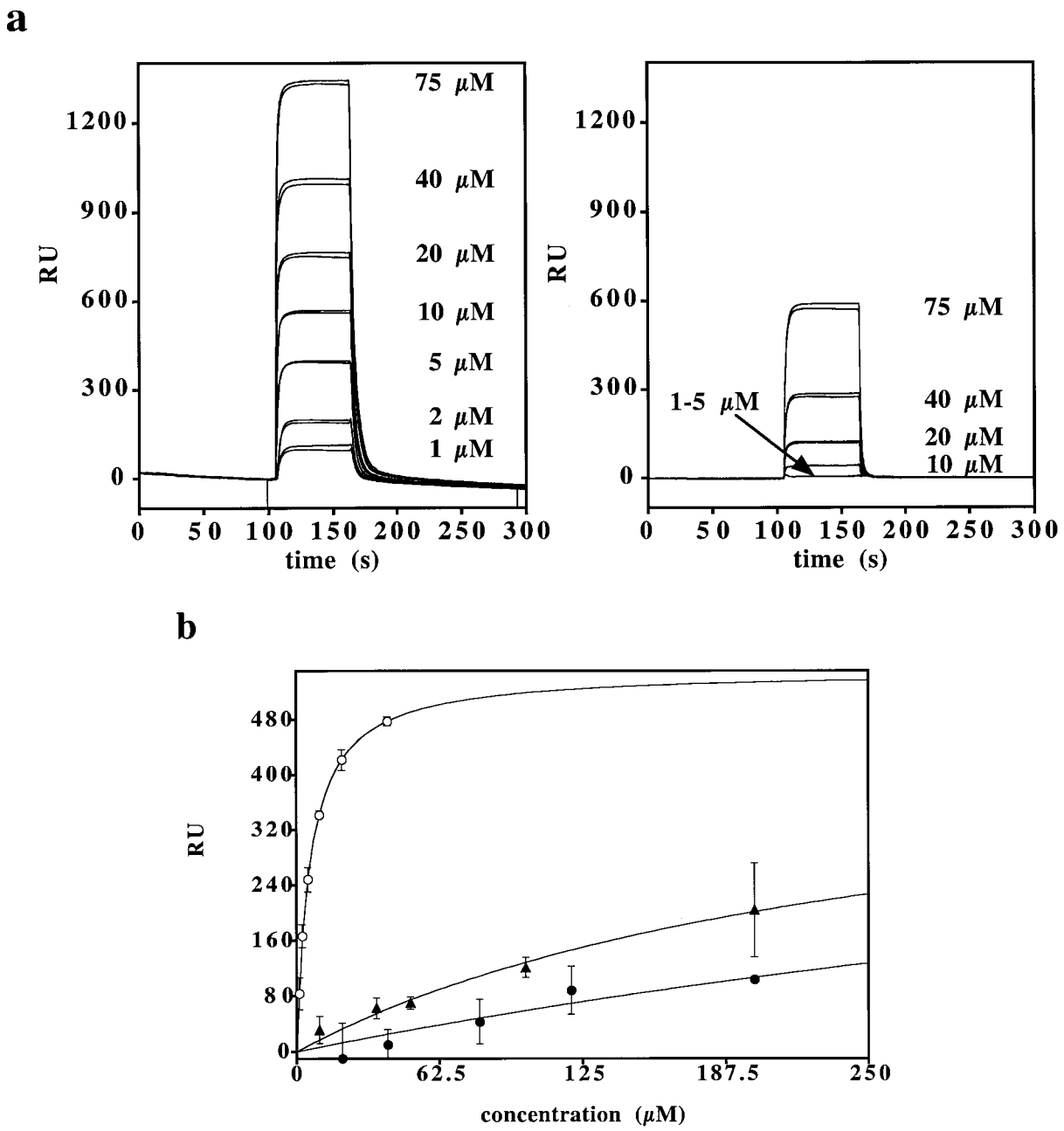

Figure 1 (*legend opposite*)

Viral escape can thus be rationalized by a dramatic loss of affinity in the transgenic T-cells consisting of the P14 TCRs to the pMHC complexes containing these epitopes on the target cells. In further agreement with our measurements, central tolerance can be induced to some degree in mice neonatally infected with the V3L-epitope containing virus variant (Pircher *et al.*, 1991), indicating that the P14 TCR must interact, albeit weakly, with the pMHC containing this epitope. In contrast, target cells pulsed with either of the viral escape epitopes are not lysed by the P14 CTLs (Pircher *et al.*, 1990) (Table 1), consistent with different thresholds of naive T-cells for negative selection and mature T-cells for activation, when APLs are presented to the T-cells (Sloan-Lancaster & Allen, 1996; Bachmann *et al.*, 1997; Germain & Stefanova, 1999).

Binding of epitope variants at position 4

In order to put the affinities determined for the pMHCs containing the viral escape epitopes in perspective, we set out to measure the affinity of pMHCs containing other altered peptide ligands, which had been studied for the P14 TCR in cellular assays (Bachmann *et al.*, 1996; Sebzda *et al.*, 1996). The results are shown in Figure 1(c) and Table 1. It is surprising that we found the Y4A-pMHC to

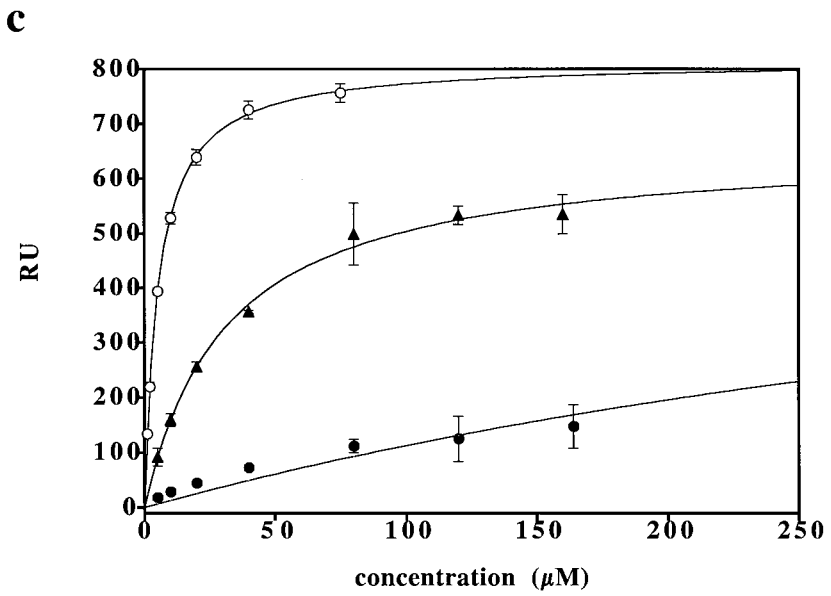

Figure 1. Binding isotherms of the P14 TCR to pMHC. (a) Binding traces of the gp33-pMHC injected over the P14-TCR surface (left panel) and reference surface (right panel). Functional TCR is immobilized non-covalently by interacting with an anti-Cβ monoclonal antibody and replaced after each regeneration. Two measurements are shown for each concentration of pMHC injected. On the right panel, the traces obtained for the concentrations of 1-5 μM pMHC injected over the reference surface generated a very low signal and are on top of each other. (b) Binding isotherm of the wt (open circles), V3L- (filled triangles) and Y4F-pMHCs (filled circles) to the P14 TCR, immobilized indirectly on the sensorchip. The error bars were calculated from two measurements. The three pMHCs were measured using the same batch of TCR on the same anti-Cβ monoclonal antibody-derivatized sensor chip. The curves were fitted to a hyperbolic binding curve (equivalent to a Scatchard plot), as described in Materials and Methods. The fit to the data of the Y4F-pMHC was obtained by taking the average value of RU_{max} obtained with four different pMHCs, as described in Results, on the same surface and using the same batch of TCR. Each dissociation constant was measured in two independent experiments. An RU_{max} of 550 for the wild-type is obtained from the fit, and the highest experimentally determined point is at 87 % saturation. (c) Binding isotherm of the wt- (open circles) , Y4A- (filled triangles) and Y4S-pMHCs (filled circles). The three pMHCs were measured using the same batch of TCR on the same anti-Cβ monoclonal antibody-derivatized sensor chip. The curves were fitted to a hyperbolic binding curve, as described in Materials and Methods. The fit to the data of the Y4S-pMHC was obtained by taking the average value of RU_{max} obtained with the Y4A- and wt-pMHC, as described in Results, on the same surface and using the same batch of TCR. Each dissociation constant was measured in two independent experiments. An RU_{max} of 814 for the wild-type is obtained from the fit, and the highest experimentally determined point is at 93 % saturation.

have a much higher affinity than the Y4F-pMHC for the P14 TCR, even though replacement of a tyrosine by an alanine residue is more radical a change than the replacement by phenylalanine. Yet, the affinity of the P14 TCR to the Y4A-containing pMHC is only fivefold lower than to the wt-pMHC complex (Table 1). Target cells pulsed with this peptide can indeed be lysed by P14 T-cells, which can also be induced to proliferate, although more weakly than by target cells pulsed with the wt epitope (Sebzda *et al.*, 1996). The Y4A epitope has thus been characterized as a weak agonist.

Current models of T-cell activation emphasize the importance of the off-rate of the TCR-pMHC interaction in discriminating between the pharmacological properties of the peptide ligands of the MHC. Assuming that the mutations in the epitopes do not significantly affect the on-rate of the TCR-pMHC interaction, a fivefold decrease in affinity would result approximately in a fivefold increase in off-rate, a difference shown by others to be sufficient to turn an agonist peptide into a weak agonist or even an antagonist (Davis *et al.*, 1998).

In contrast, we only detected a weak signal when injecting the Y4S-pMHC on the P14 surface (Figure 1(c)). As we did for the Y4F-pMHC, we tried to estimate the K_D for this APL by constraining RU_{max} to the average obtained on the same chip with the same batch of TCR for the Y4A and the wt-pMHC. We estimated a K_D of 530 μM by this procedure (Table 1). The very low level of binding showed, however, some saturation at low RUs, and we cannot fully exclude that the pMHCs containing this epitope would recognize a minor alternative conformation of the P14 TCR, not equilibrating with the main conformation. This would result in a higher level of affinity of this pMHC to this type of minor conformer of the TCR, but in the absence of any detectable interaction to the major conformer. The Y4S-peptide has been previously shown to be an antagonist (Sebzda *et al.*, 1996). Recent work has more thoroughly characterized

Table 2. Solvent accessibility of peptide residues and interaction partners

Residue	H-bonds[a]	Hydrophobic interactions[a,b]	Accesible surface: Side-chain atoms[c] (Å^2)	Accesible surface: Main-chain atoms[c] (Å^2)	Accesible surface: % of total[c,d]
P1Lys	N→OH Tyr171 O→OH Tyr159	Glu63 Trp167	30.9	0.0	10.6
P2Ala	N→O$^{\varepsilon 1}$ Glu63 O→N$^{\zeta}$ Lys66	Tyr7 Lys66	2.3	1.0	1.1
P3Val	O→O$^{\varepsilon 2}$ Glu9[e]	Tyr159	0.8	0.0	0.3
P4Tyr	O→N$^{\varepsilon 2}$ His155	Lys66	112.0	2.4	39.3
P5Asn	N → O$^{\varepsilon 1}$ Gln70 N$^{\delta 1}$→N$^{\varepsilon 2}$ Gln97 N$^{\delta 2}$→N$^{\varepsilon 1}$ Gln97	Trp73	0.0	12.8	4.4
P6Phe	N→OH Tyr156 O→N$^{\varepsilon 1}$ Trp73	His155 Ala152	62.9	15.2	26.8
P7Ala	O→OH Tyr156[e]	Trp147	10.2	10.0	6.9
P8Thr	O→N$^{\varepsilon 1}$ Trp147 O→N$^{\zeta}$ Lys146 O$^{\gamma 1}$→N$^{\zeta}$ Lys146	Trp73	26.5	3.9	10.5
P9Cys	N→l O$^{\gamma}$ Ser77 OT1→O$^{\gamma 1}$ Thr143 OT1→OH Tyr84 OT2→N$^{\delta 2}$ Asn80 OT2→N$^{\zeta}$ Lys146	Trp73 Ser77	0.0	0.0	0.0

[a] As identified by the program HBPLUS (McDonald & Thornton, 1994), using default parameters.
[b] Only for side-chains, and defined as carbon or sulfur atoms in contact with other carbon or sulfur atoms.
[c] Calculated using the program Surface (Collaborative Computational Project Number 4, 1994), using a 1.4 Å probe.
[d] Ratio between the accessible surface of a whole residue and the total accessible surface of the peptide.
[e] Hydrogen bonds mediated by an ordered water molecule.

the mechanism of action of this peptide, and shown that it antagonizes T-cell proliferation and TCR down-regulation at high concentration and in high molar excess over the wt peptide (Bachmann *et al.*, 1998). In fact, Y4S was postulated to be the peptide leading to the weakest interaction between P14 TCR and pMHC out of a series of antagonists. This is in agreement with the low affinity we have found for the interaction between the Y4S-pMHC and P14 TCR.

We have included another peptide, the F6Y/T8S double mutant epitope, in our analysis (Table 1). This epitope was shown to be able to induce the full spectrum of T-cell responses, although somewhat more weakly than the wt epitope (Bachmann *et al.*, 1996). We have found a twofold lower affinity of the P14 TCR for the pMHC containing this epitope. In summary, we find a strong correlation between the affinity of the P14 TCR for the pMHCs containing the APLs, and the corresponding T-cell responses induced by these ligands, as well as with their classification as agonist, weak agonist or antagonist (Table 1), (Pircher *et al.*, 1990; Bachmann *et al.*, 1996; Sebzda *et al.*, 1996).

Crystal structure of the pMHC complex

We determined the pMHC structure with wt gp33c peptide, KAVYNFATC, at 2.75 Å resolution in the spacegroup $P2_1$ (Figure 2(a) and (b), Table 3). The overall structure of H-2D^b is very similar to the published structure of H-2D^b with the influenza virus np366 peptide ASNENMETM (Young *et al.*, 1994). Superposition of the C$^{\alpha}$ atoms of the $\alpha 1/\alpha 2$ domains in the two structures gives a rmsd of 0.55 Å. The gp33c peptide, shown in Figure 2(b) with its electron density, adopts an extended conformation and arches at P6 and P7 over the MHC due to the presence of a hydrophobic ridge which cuts across the binding site (Figure 2(b)) (Young *et al.*, 1994). Side-chains P1, P4, P6, P7 and P8 are solvent accessible, and thus available for interaction with the TCR (Figure 2(a) and (b)), while side-chains P2, P3, P5 and P9 are buried in pockets of the H-2D^b binding cleft (Figure 2(a) and (b)). The solvent-accessible surface of each peptide side-chain and their interactions with MHC residues are listed in Table 2 (Collaborative Computational Project Number 4, 1994; McDonald & Thornton, 1994).

It is worth mentioning that modeling of the gp33 peptide in the H-2D^b-binding cleft (Lewicki *et al.*, 1995), based on the np366/H-2D^b crystal structure (Young *et al.*, 1994), had allowed the prediction of the solvent-exposed residues, and the identification of their approximate orientation. On the other hand, in the modeled structure Lewicki *et al.* (1995) drastically changed the P6 Ψ dihedral angle to allow for the Met to Phe substitution, and avoid a clash with the walls of the binding site. Our X-ray structure shows instead that such a change happens to a much smaller extent; rather, the bulkier Phe side-chain is accommodated in a minor shallow pocket on the H-2D^b surface (Figure 2(a)), and the main-chain is shifted towards the $\alpha 2$-helix. As a result, the distance between the two P6 C$^{\alpha}$ atoms, after superimposing the $\alpha 1/\alpha 2$ domains, is 1.45 Å.

Superposition of the gp33c peptide with the two other peptides containing the canonical anchor Asn

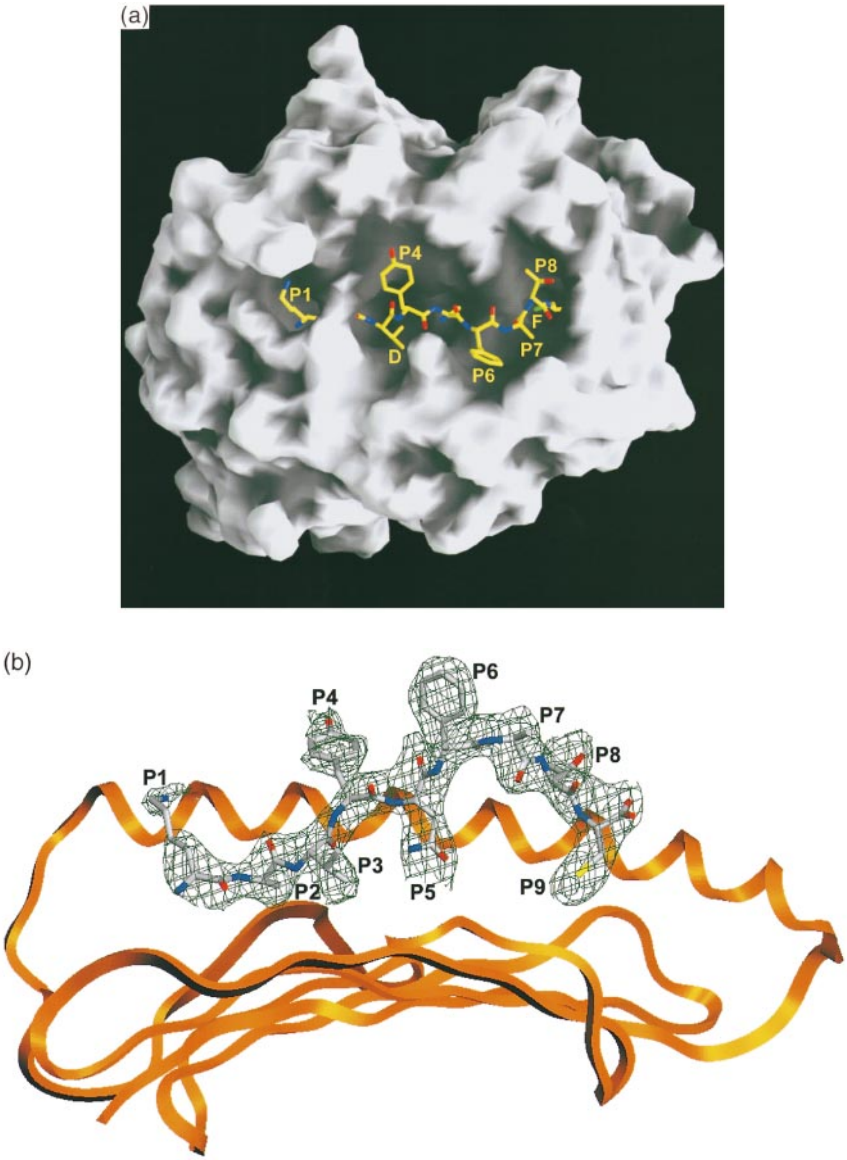

Figure 2. H-2D^b peptide-binding groove. (a) Surface representation of the H-2D^b-binding groove; the bound gp33c peptide is shown with the main chain running from left to right. The labels show the solvent exposed residues of the peptide, and the positions of the D and F pockets in the MHC molecule. Picture generated with GRASP (Nicholls *et al.*, 1991). (b) Side view of gp33c bound to H-2D^b. The view is from the α2-helix side of the MHC class I heavy chain. The α1-helix lies behind the peptide, and the α2-helix has been removed for clarity. The β-sheet forms the floor of the binding site. The $2F_o - F_c$ map is contoured at 1.2 σ level. Figure 2(b) was generated with SETOR (Evans, 1993).

in position P5 (Falk *et al.*, 1991) in complex with H-2D^b, namely the above-mentioned np366 peptide (Young *et al.*, 1994) and the Sendai virus peptide FAPGNYPAL (Glithero *et al.*, 1999) (Figure 3(a)), gives comparable rms deviation values for the C^α atoms. These values vary from 0.58 Å for the np366-Sendai virus pair, 0.75 Å for the gp33c-np366 pair, and finally to 0.90 Å for the gp33c-Sendai virus pair. The highest rms distance is observed for the P6 residue, ranging from 1.45 Å to 2.30 Å for the three pairwise comparisons. All the above-mentioned values are calculated after superimposing the α1/α2 H-2D^b domains. This striking conformational variability at P6 is confirmed by an analysis of the ϕ-ψ dihedral angles. The value of ϕ for P6 varies between −107° and −89°, while ψ varies from −124° to −42°: this is the highest variation found for the nine peptide residues. Furthermore, despite the similarity between the two P6 side-chains Phe and Tyr, in the gp33c and Sendai virus peptides, respectively, these residues contribute a considerably different portion of the total solvent exposed surface of the respective peptides: 78 Å^2 out of a total of 291 Å^2 (27 %) for gp33c (Table 2), and 148 Å^2 out of 256 Å^2 (58 %) for the Sendai virus.

Our analysis suggests that the presence of the hydrophobic ridge has the effect of locally increas-

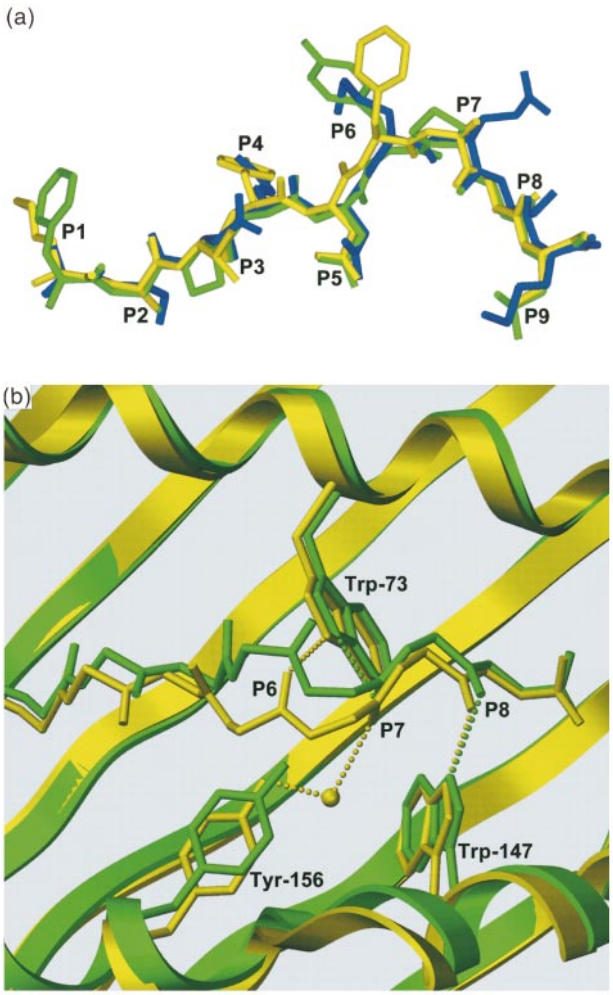

Figure 3. Comparative analysis of viral peptides bound to H-2D^b. (a) Superposition, based on the C$^\alpha$ positions of the α1α2 MHC domains, of the gp33c peptide (KAVYNFATC, yellow), np366 influenza virus peptide (ASNMETM, blue) and Sendai virus peptide (FAPGNYPAL, green). (b) The hydrophobic ridge of H-2D^b. The superposition of the gp33c- (yellow) and Sendai virus- (green) pMHCs, based on the C$^\alpha$ positions of the α1α2 MHC domains, shows the different network of hydrogen bonds formed by the hydrophobic ridge residues. The two structures are seen from the solvent accessible side, with both peptide main-chains running from left to right. The hydrogen bonds are represented as broken lines, and the water molecule as a sphere. Figure 3 was generated with SETOR (Evans, 1993).

ing the variability of the peptide conformation. The hydrophobic ridge is comprised of residues Trp73, Trp147 and Tyr156. Trp147 N$^{\varepsilon 1}$ forms a conserved hydrogen bond with the main-chain carbonyl oxygen atom of P8 in all three structures (Figure 3(b)); however, a different hydrogen bond pattern occurs with the other two residues. Trp73 N$^{\varepsilon 1}$ is hydrogen-bonded to the P6 main-chain carbonyl oxygen atom in the gp33c structure, but rather binds to the P7 main-chain oxygen atom in the other two structures. Conversely, the P7 main-chain oxygen atom of gp33c makes an additional interaction, *via* a water molecule, with the hydroxyl group of Tyr156 (Figure 3(b)).

Table 3. Crystallographic parameters

A. *Cell parameters* (Spacegroup $P2_1$)	
a (Å)	92.53
b (Å)	124.77
c (Å)	99.56
α (deg.)	90
β (deg.)	103.03
γ (deg.)	90
No. molecules per asymmetric unit	4
B. *Data collection*	
Resolution limits (Å)	29.8-2.75
No. unique reflections[a]	51,494 (3331)
Redundancy[a]	2.7 (2.3)
Completeness[a] (%)	90.8 (88.4)
Average I/σ[a]	11.7 (2.0)
R_{merge} [a]	8.0 (38.6)
C. *Refinement*	
R_{factor} [b] (%)	23.6
R_{free} [c] (%)	27.6
No. water molecules	114
Rmsd bonds (Å)	0.009
Rmsd angles (deg.)	1.46

[a] Numbers in parenthesis refer to the outermost resolution shell 2.81-2.75 Å.
[b] 46,277 reflections.
[c] 5197 reflections.

In the structure of H-2D^b in complex with the np366 peptide from influenza virus (Young *et al.*, 1994), the F pocket (Saper *et al.*, 1991) is occupied by a Met residue in position P9, while our structure contains a Cys residue at this position. Both side-chains contribute hydrophobic interactions to the overall binding. The larger Met side-chain reaches to the end of the pocket, interacting with Phe116, while the Cys side-chain interacts with Ser77 at the rim of the pocket (Figure 4(a)). Three hydrogen bonds between the peptide C-terminal carboxylate group and the H-2D^b residues Asn80, Tyr84, and Thr143 are conserved. The rms distance for the C$^\alpha$ of the two residues (0.12 Å) clearly demonstrates that the peptide conformation at the C terminus is independent of the presence of Cys or Met in P9, and thus both residues can be used interchangeably, as can be seen from their structural superposition (Figure 4(a)). Careful visual inspection of the B, C, D and F pockets in the structure, and comparison with the two other structures of H-2D^b (Young *et al.*, 1994; Glithero *et al.*, 1999) using the program O (Jones *et al.*, 1991), did not reveal significant structural changes of the side-chains lining these pockets, but mere local rearrangements.

Discussion

Recognition of gp33-pMHC by P14 TCR

A striking feature of the interaction between the gp33-pMHC and the P14 TCR is the strong dependence of the affinity on the nature of the residue at

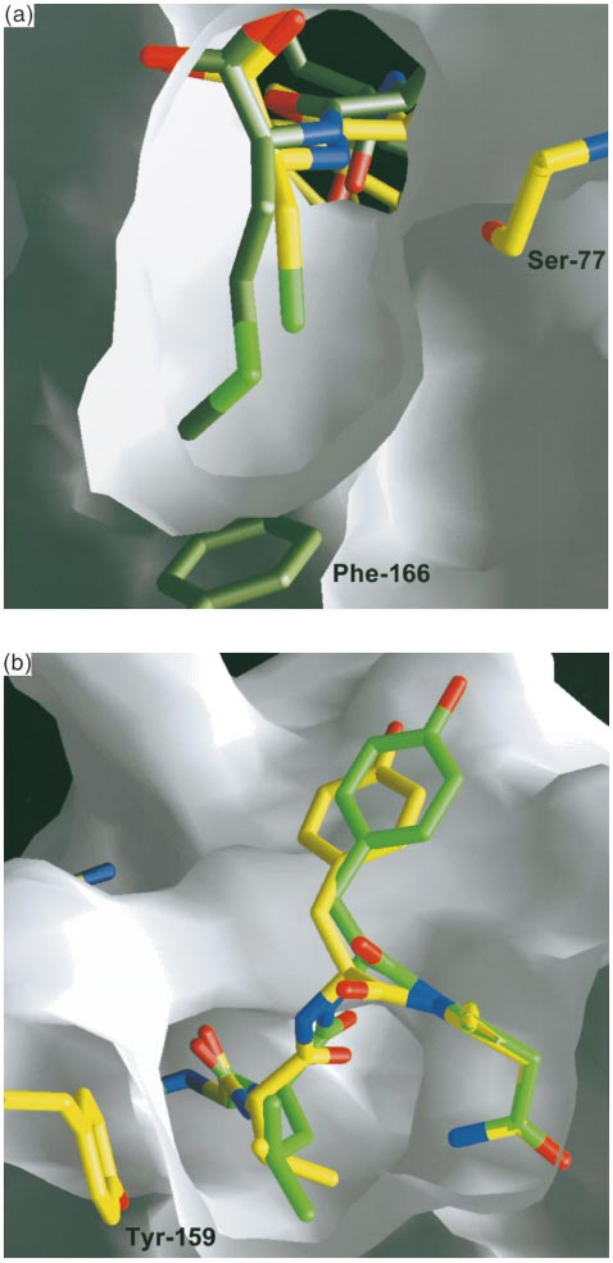

Figure 4. View of the D and F pockets from the H-2D^b/gp33c structure. (a) The F pocket is seen from the distal side of the binding groove. The influenza virus peptide np366 (olive green) has been superimposed onto the gp33c peptide (yellow), and shown here are the P9 residues from the above-mentioned peptides. Ser77 from the H-2D^b/gp33c structure, and Phe116 from the H-2D^b/np366 structure are also shown, after superposition of the binding sites. (b) Cross-sectional view of the D pocket. The gp33c peptide is shown in yellow, as well as Tyr159 (far left). The simulated V3L peptide is shown in green. The molecular surface of the MHC class I molecule is shown in arbitrary colors, and was produced using GRASP (Nicholls *et al*., 1991).

position 4. This residue is freely accessible for the TCR, as seen in the structure (Figure 2(a)), and contributes the most to the accessible surface of the peptide (Table 2), which is in agreement with its predominance in the interaction between the P14 TCR and the gp33-pMHC. Although it is common for pMHC-TCR interactions to be dominated by the contribution of only a few residues (Garcia *et al*., 1999), we have here the extreme case where removal of a single hydroxyl group, by introducing a phenylalanine for a tyrosine residue, completely abolishes the interaction with a hundred-fold reduction in affinity. It is more surprising that the far less conservative replacement of tyrosine by an alanine residue leads to a much smaller reduction in affinity, while substitution of the tyrosine residue to serine also shows a dramatic reduction in binding. Although no quantitative binding data are available, a tyrosine to valine substitution at this position has also been investigated (Bachmann *et al*., 1998). The data on cell lysis or T-cell proliferation obtained for this ligand show also the typical pattern of a weak interaction, much weaker than for the alanine substituted peptide (Bachmann *et al*., 1998). Tyr at position 4 is therefore best replaced by alanine. This suggests that the TCR finds an alternate mode of binding to the pMHC with Ala at position 4 which cannot be explained by a static picture. The generation of unsatisfied hydrogen bond partners and steric constraints or induced fit are likely to play a major role. This is in agreement with the concept of a ''functional hot spot'', as demonstrated in the crystal structure of the complex of the 2C TCR and the SIYR/H-2 K^b pMHC (Degano *et al*., 2000).

On the other hand, we do not find such a strong dependence of the interaction on the residues at position 6 and 8, which are facing outwards in the structure as well (Figure 2(a), Table 2), since the F6Y/T8S peptide leads only to a small decrease in affinity of the corresponding pMHC for the P14 TCR. However, there might be compensating effects between the two sites, and a more detailed analysis would be needed to assess the importance of these side-chains for the interaction with the TCR. Lewicki *et al*. (1995) found a complete abrogation of CTL lysis when introducing single alanine residue substitutions at position 6 and 8 in the gp33 epitope, strongly suggesting their importance in TCR recognition.

Structural alignment of a homology model of the P14 TCR (A. Honegger, unpublished results) and the structure of the gp33c-pMHC with the two published TCR-pMHC complexes resulted in numerous clashes between TCR and pMHC atoms. The pMHCs were aligned on the conserved α1 and α2-helices, and the TCRs on their framework residues. The way a TCR interacts with a pMHC of known structure is therefore too intricate and complex to be predicted by a simple structural alignment procedure, and the structure has to be solved each time.

Substituting valine for leucine at position 3 of the peptide also leads to a dramatic decrease in affinity for the TCR (Table 1, Figure 1(b)), although residue 3 is buried within the MHC (Figures 2(b),

4(b)). Val3 binds to the D pocket of H-2D^b, according to the nomenclature by Saper *et al*. (1991). This pocket is lined by Ser99, Leu114, Tyr156, and Tyr159, and is mostly hydrophobic in nature, with the interaction between the peptide and the protein being dominated by the hydrophobic contact between P3Val and Tyr159 (Figure 4(b)). The substitution of Val to the bulkier Leu residue most probably leads to a clash with the pocket residues and induces a shift of the peptide chain, which in turn alters the interaction with the TCR. This was tested by introducing the relevant mutation into the experimental structure, and carrying out a conjugate gradient minimization using CNS (Brünger *et al*., 1998), excluding the experimental energy terms and allowing the pocket residues as well as the P2 to P4 peptide residues to move (Figure 4(b)). Small but significant movements of the peptide backbone and side-chains were revealed (Figure 4(b)). Overall, these rearrangements in the pMHC-complex explain the 50-fold reduction in affinity to the TCR.

Mutations in the virus which lead to escape from the immune system, most likely abolish recognition by two mechanisms in our case: either by affecting a residue directly in contact with the TCR, in our case residue P4, or by affecting more indirectly recognition through conformational changes in the peptide or the MHC. These two mechanisms have been demonstrated in crystallographic studies on pMHC and TCR-pMHC complexes containing altered peptide ligands (Reid *et al*., 1996; Ding *et al*., 1999). Here, we have been able to quantify the effect of these structural changes on the affinity of the interaction between TCR and pMHC containing viral escape epitopes.

Using the V3L epitope an interesting phenomenon was observed which had originally been described for antibodies, termed the ''original antigenic sin'' (Klenerman & Zinkernagel, 1998). Mice primed with the virus carrying the wt epitope respond to a subsequent infection with viruses carrying the variant epitope with a CTL response targeting the wt epitope, rather than the variant epitope (Klenerman & Zinkernagel, 1998). By providing a measure of the affinity of the pMHC carrying this ligand to the P14 TCR, we show here that, although the affinity of the TCR for this pMHC is reduced 50-fold compared to the pMHC containing the wt epitope (Table 1), a specific interaction still occurs. This would support the interpretation proposed by Klenerman & Zinkernagel (1998) that the interaction between the TCRs recognizing the wt peptide and pMHCs carrying the variant ligand would still result in positive selection of thymocytes directed against the wt epitope, and may also provoke CTL expansion in the periphery.

Antagonist ligands

T-cell activation is thought to be controlled by the kinetics of the TCR-pMHC interaction, whereby the off-rate of this interaction discriminates between an agonist, weak agonist or antagonist peptide (Davis *et al*., 1998; Grakoui *et al*., 1999). Antagonist ligands have been postulated to interfere with the productive clustering of the signaling TCRs, thereby either preventing the accumulation of positive signals, or even inducing negative signals (Germain & Stefanova, 1999). pMHCs on APCs have been found to serially engage and activate TCRs, leading to their down-modulation (Valitutti *et al*., 1995). In this context, antagonism has been suggested to act by reducing the amount of TCRs available for signaling below a certain critical threshold (Lanzavecchia *et al*., 1999). Furthermore, a hierarchy of T-cell activation has been observed, where responses such as cytotoxicity or T-cell proliferation for a given ligand have been shown to have different requirements in terms of ligand concentration (Sloan-Lancaster & Allen, 1996; Valitutti *et al*., 1996; Bachmann *et al*., 1997; Germain & Stefanova, 1999).

Recently, Grakoui *et al*. (1999) have shown, using the cluster density of pMHCs as a readout, that this parameter correlated best with the half-life of the TCR-pMHC interaction determined by BIACORE, when comparing data from two different TCR systems. They used an experimental set-up in which T-cells interacted with pMHCs embedded in a glass-supported planar bilayer. Within one TCR system, cluster density also correlated with the dissociation constant. This indicates that the mutations within the peptide ligands primarily affect off-rates and the on-rates are therefore rather constant, as is typical for most protein-ligand interactions. Consistent with these findings, the 50-fold and 100-fold reductions in affinity of the viral escape mutants found here would also be expected to correspond to an equivalent increase in off-rate, explaining the lack of T-cell response found for these peptide ligands. The APL Y4A has been classified as a weak agonist. We have found only a fivefold decrease in the level of affinity for the TCR. The relatively high affinity of the pMHC containing this peptide is reflected well in cellular assays for antagonism, where high concentrations of this ligand do not inhibit T-cell proliferation or cytotoxicity but rather increase it, showing that this ligand is not an antagonist (Bachmann *et al*., 1998). As the Ala4-containing peptide has a far higher level of affinity than any other mutation at this position, we must conclude that the introduction of the minimal-length alanine side-chain does not induce a conformational disturbance of the complex, in contrast to other residues.

Conclusions

We provide, for the first time, a measure of the affinity between pMHCs containing viral escape ligands and their TCR. We have characterized two types of escape epitopes. One is a null ligand (Y4F), while the other (V3L) is still able to induce

central tolerance to some extent, and may as well provoke CTL expansion in the periphery. Furthermore, we provide affinity data on weak agonist and antagonist ligands with which the viral escape ligands can be compared. We find that these ligands are within the affinity range expected for antagonist or null peptides. In this respect, it will be interesting to find out whether the viral escape epitopes analyzed here can function as antagonists of the wt ligand, and if so, whether they act only when in excess over the wt ligand or already substoichiometrically. In summary, agonists, weak agonists and antagonists are peptides which are characterized by the magnitude of interaction energy (reflected in affinity and off-rate). Below a critical threshold, sufficient TCR clustering can no longer occur. The virus, however, has several options to achieve this type of mutation. A variant can be selected which directly targets the most exposed residue, or which can disturb the interaction of the peptide with the MHC. In this respect, alteration of epitope side-chains interacting with small pockets of the MHC are more likely to result in escape than truncation of side-chains interacting with large pockets. It appears that a reduction in affinity to about 500 μM K_D provides a safe viral escape, which can be achieved with a variety of single point mutations.

Materials and Methods

The peptides were synthesized and purified by Chiron Technologies (Clayton Victoria, Australia) to 95 % purity and analyzed by mass spectrometry. The peptides had the following sequences: gp33-41 (gp33): KAVYNFATM, gp33-41 with Cys-9 instead of Met-9 (gp33c): KAVYNFATC, gp33-41 V3L (V3L): KALYNFATM, gp33-41 Y4A (Y4A): KAVANFATM, gp33-41 Y4F (Y4F): KAVFNATM, gp33-41 Y4S (Y4S): KAVSNFATM, gp33-41 F6Y/T8S (F6Y/T8S): KAVYNYASM. The plasmids encoding H-2D^b and β_2-microglobulin (Young *et al.*, 1994) were obtained from Dr J. C. Sacchettini (Department of Biochemistry, Albert Einstein College of Medicine, New York).

Expression and purification of TCR and pMHC

The TCR and pMHC complexes were expressed, refolded and purified as described by Tissot *et al.* (2000). The TCR was refolded by dialysis against 20 volumes of 0.4 M arginine-HCl, 20 mM Tris-HCl (pH 8.0) and subsequently dialyzed against 20 mM Tris-HCl, 150 mM NaCl (pH 8.0). It was then purified by three runs of gel filtration over a Superdex G200 column (Amersham Pharmacia Biotech) (Tissot *et al.*, 2000).

The pMHCs were refolded as described, except for the gp33-pMHC with cysteine, which was refolded in a buffer containing 0.8 M arginine-HCl, 200 mM Tris-HCl, 2 mM EDTA, 1 mM oxidized L-glutathione and 5 mM reduced L-glutathione (pH 7.5). Except for the MHC/gp33c complex, which was purified by anion exchange chromatography (Tissot *et al.*, 2000), all of the pMHCs were purified by two runs of gel filtration on a Superdex G-75 column (Amersham Pharmacia Biotech). The protein concentrations were determined by spectrophotometry (Gill & von Hippel, 1989).

Surface plasmon resonance

All measurements were performed on a BIACORE instrument (BIACORE AB, Uppsala, Sweden) as described by Tissot *et al.* (2000). In brief, the TCR was non-covalently bound to the anti-Cβ antibody H57-597 (Kubo *et al.*, 1989), which in turn was covalently derivatized on the chip. Both the TCR-containing surface and control surfaces were regenerated with 0.1 M glycine/HCl, 500 mM NaCl (pH 2.5) after each injection. The signal was calculated by subtracting the signal obtained on a deactivated control surface from the signal obtained on the TCR surface. Each data point was the average of two measurements. The dissociation constant was obtained by plotting (KaleidaGraph 3.08, Synergy Software, Reading, PA) the signal in RUs against the concentration of the injected pMHC, and fitting it to a hyperbolic curve, $RU = RU_{max} \times [\text{pMHC}]/(K_D + [\text{pMHC}])$, where RU_{max} is the maximal value at saturation. Each dissociation constant was measured in two independent experiments.

Crystallization, X-Ray data collection, structure solution, and refinement

Crystals of the H-2D^b/gp33c complex were grown by the hanging drop vapor diffusion method at 4 °C. Two microliters of protein solution, containing a 1:1 molar ratio of MHC/peptide (at a total protein concentration of 5.85 mg/ml), was mixed with 1 μl of reservoir solution; the reservoir solution contained 0.1 M ammonium sulfate, 20 % (w/v) PEG 4000, 0.1 M Hepes buffer (pH 7.4), and 0.02 % (w/v) sodium azide. Prior to data collection, the crystals were transferred into a buffer containing the reservoir solution enriched with 20 % (v/v) glycerol, and flash-frozen in a stream of liquid nitrogen at a temperature of 100 K. A 91 % complete dataset at 2.75 Å resolution was collected from a single crystal, using an Enraf Nonius CuK_α rotating anode X-ray source, equipped with double focusing mirrors (MacScience). The data were processed and scaled using the HKL suite of programs (Otwinowski & Minor, 1997). The crystals belong to the primitive monoclinic spacegroup $P2_1$. Structure determination was carried out using the molecular replacement method with the program AMoRe (Navaza, 1994), using the H-2D^b/p1027 complex (Zhao *et al.*, 1999) (RCSB Protein Data Bank code 1bz9) as a search model, after removal of the peptide. The structure solution indicated the presence of four complexes in the asymmetric unit. Two strong cross-rotation function peaks were found, and the subsequent translation function search detected a total of four strong peaks. These peaks identified four molecules, two of which had independent orientations, while the other two were related to the first pair by simple translation. Fast rigid-body refinement of the four solutions of the rotational and translational search gave a correlation coefficient of 57.4 %, and an R_{factor} of 48.8 %. Independent rigid-body refinement of the heavy chain and β_2-microglobulin was then performed using CNS (Brünger *et al.*, 1998). Afterwards, cycles of structure refinement in CNS, using strong non-crystallographic symmetry restraints (300 kcal mol^{-1} Å^{-2}), were alternated with manual rebuilding of the model in O (Jones *et al.*, 1991). Simulated annealing was utilized in the early stages of refinement. The peptide was introduced as a poly-alanine model after the R_{factor}

and R_{free} had decreased below 28 % and 30 % respectively, and the appropriate residues were introduced in later stages. Grouped *B*-factor refinement was initially performed using one value per residue, and towards the end of refinement two *B* values were refined, one for the backbone atoms and one for the side-chain atoms. Fourfold non-crystallographic symmetry average maps produced with the program DM (Cowtan, 1994) were used throughout the model-building process. The final R_{factor} and R_{free} were 23.6 % and 27.6 %, respectively. The crystallographic statistics are presented in Table 3.

Acknowledgments

We thank Dr G. Capitani and M. Donepudi for valuable suggestions, Dr A. Honegger for modeling the P14 TCR, and Dr R. M. Zinkernagel and Dr H. Hengartner for helpful discussions and critical reading of the manuscript.

References

Bachmann, M. F., Sebzda, E., Kündig, T. M., Shahinian, A., Speiser, D. E., Mak, T. W. & Ohashi, P. S. (1996). T-cell responses are governed by avidity and co-stimulatory thresholds. *Eur. J. Immunol.* **26**, 2017-2022.

Bachmann, M. F., Oxenius, A., Speiser, D. E., Mariathasan, S., Hengartner, H., Zinkernagel, R. M. & Ohashi, P. S. (1997). Peptide-induced T-cell receptor down-regulation on naive T-cells predicts agonist/partial agonist properties and strictly correlates with T-cell activation. *Eur. J. Immunol.* **27**, 2195-2203.

Bachmann, M. F., Speiser, D. E., Zakarian, A. & Ohashi, P. S. (1998). Inhibition of TCR triggering by a spectrum of altered peptide ligands suggests the mechanism for TCR antagonism. *Eur. J. Immunol.* **28**, 3110-3119.

Bertoletti, A., Sette, A., Chisari, F. V., Penna, A., Levrero, M., De Carli, M., Fiaccadori, F. & Ferrari, C. (1994). Natural variants of cytotoxic epitopes are T-cell receptor antagonists for antiviral cytotoxic T-cells. *Nature,* **369**, 407-410.

Borrow, P. & Shaw, G. M. (1998). Cytotoxic T-lymphocyte escape viral variants: how important are they in viral evasion of immune clearance *in vivo*? *Immunol. Rev.* **164**, 37-51.

Brünger, A. T., Adams, P. D., Clore, G. M., DeLano, W. L., Gros, P., Grosse-Kunstleve, R. W., Jiang, J. S., Kuszewski, J., Nilges, M., Pannu, N. S., Read, R. J., Rice, L. M., Simonson, T. & Warren, G. L. (1998). Crystallography and NMR system: a new software suite for macromolecular structure determination. *Acta Crystallog. sect. D,* **54**, 905-921.

Collaborative Computational Project Number 4 (1994). The CCP4 suite: programs for protein crystallography. *Acta Crystallog. sect. D,* **50**, 760-763.

Cowtan, K. (1994). *Joint CCP4 and ESF-EACBM Newsletter on Protein Crystallography*, **31**, 34-38.

Davis, M. M., Boniface, J. J., Reich, Z., Lyons, D., Hampl, J., Arden, B. & Chien, Y. (1998). Ligand recognition by alpha beta T-cell receptors. *Annu. Rev. Immunol.* **16**, 523-544.

Degano, M., Garcia, K. C., Apostolopoulos, V., Rudolph, M. G., Teyton, L. & Wilson, I. A. (2000). A functional hot spot for antigen recognition in a superagonist TCR/MHC complex. *Immunity,* **12**, 251-261.

Ding, Y. H., Baker, B. M., Garboczi, D. N., Biddison, W. E. & Wiley, D. C. (1999). Four A6-TCR/peptide/HLA-A2 structures that generate very different T-cell signals are nearly identical. *Immunity,* **11**, 45-56.

Evans, S. V. (1993). SETOR: hardware-lighted three-dimensional solid model representations of macromolecules. *J. Mol. Graph.* **11**, 134-138, 127-138.

Falk, K., Rotzschke, O., Stevanovic, S., Jung, G. & Rammensee, H. G. (1991). Allele-specific motifs revealed by sequencing of self-peptides eluted from MHC molecules. *Nature,* **351**, 290-296.

Garboczi, D. N., Ghosh, P., Utz, U., Fan, Q. R., Biddison, W. E. & Wiley, D. C. (1996). Structure of the complex between human T-cell receptor, viral peptide and HLA-A2. *Nature,* **384**, 134-141.

Garcia, K. C., Teyton, L. & Wilson, I. A. (1999). Structural basis of T-cell recognition. *Annu. Rev. Immunol.* **17**, 369-397.

Germain, R. N. & Stefanova, I. (1999). The dynamics of T-cell receptor signaling: complex orchestration and the key roles of tempo and cooperation. *Annu. Rev. Immunol.* **17**, 467-522.

Gill, S. C. & von Hippel, P. H. (1989). Calculation of protein extinction coefficients from amino acid sequence data. *Anal. Biochem.* **182**, 319-326.

Glithero, A., Tormo, J., Haurum, J. S., Arsequell, G., Valencia, G., Edwards, J., Springer, S., Townsend, A., Pao, Y. L., Wormald, M., Dwek, R. A., Jones, E. Y. & Elliott, T. (1999). Crystal structures of two H-2Db/glycopeptide complexes suggest a molecular basis for CTL cross-reactivity. *Immunity,* **10**, 63-74.

Grakoui, A., Bromley, S. K., Sumen, C., Davis, M. M., Shaw, A. S., Allen, P. M. & Dustin, M. L. (1999). The immunological synapse: a molecular machine controlling T-cell activation. *Science,* **285**, 221-227.

Jones, T. A., Zou, J. Y., Cowen, S. W. & Kjeldgaard, M. (1991). Improvement methods for building protein models in electron density maps and the location of errors in these models. *Acta Crystallog. sect. A,* **47**, 110-119.

Klenerman, P. & Zinkernagel, R. M. (1998). Original antigenic sin impairs cytotoxic T-lymphocyte responses to viruses bearing variant epitopes. *Nature,* **394**, 482-485.

Klenerman, P., Rowland-Jones, S., McAdam, S., Edwards, J., Daenke, S., Lalloo, D., Koppe, B., Rosenberg, W., Boyd, D. & Edwards, A., *et al.* (1994). Cytotoxic T-cell activity antagonized by naturally occurring HIV-1 Gag variants. *Nature,* **369**, 403-407.

Kubo, R. T., Born, W., Kappler, J. W., Marrack, P. & Pigeon, M. (1989). Characterization of a monoclonal antibody which detects all murine alpha beta T-cell receptors. *J. Immunol.* **142**, 2736-2742.

Lanzavecchia, A., Lezzi, G. & Viola, A. (1999). From TCR engagement to T-cell activation: a kinetic view of T-cell behavior. *Cell,* **96**, 1-4.

Lewicki, H., Tishon, A., Borrow, P., Evans, C. F., Gairin, J. E., Hahn, K. M., Jewell, D. A., Wilson, I. A. & Oldstone, M. B. (1995). CTL escape viral variants. I. Generation and molecular characterization. *Virology,* **210**, 29-40.

McDonald, I. K. & Thornton, J. M. (1994). Satisfying hydrogen bonding potential in proteins. *J. Mol. Biol.* **238**, 777-793.

McMichael, A. (1998). T-cell responses and viral escape. *Cell,* **93**, 673-676.

Navaza, J. (1994). AmoRe: an automated package for molecular replacement. *Acta Crystallog. sect. A,* **47**, 110-119.

Nicholls, A., Sharp, K. A. & Honig, B. (1991). Protein folding and association: insights from the interfacial and thermodynamic properties of hydrocarbons. *Proteins: Struct. Funct. Genet.* **11**, 281-296.

Otwinowski, Z. & Minor, W. (1997). Processing of X-ray diffraction data collected in oscillation mode. *Methods Enzymol.* **276**, 307-326.

Pircher, H., Moskophidis, D., Rohrer, U., Bürki, K., Hengartner, H. & Zinkernagel, R. M. (1990). Viral escape by selection of cytotoxic T cell-resistant virus variants *in vivo*. *Nature,* **346**, 629-633.

Pircher, H., Brduscha, K., Steinhoff, U., Kasai, M., Mizuochi, T., Zinkernagel, R. M., Hengartner, H., Kyewski, B. & Müller, K. P. (1993). Tolerance induction by clonal deletion of $CD4^+8^+$ thymocytes *in vitro* does not require dedicated antigen-presenting cells. *Eur. J. Immunol.* **23**, 669-674.

Pircher, H., Rohrer, U. H., Moskophidis, D., Zinkernagel, R. M. & Hengartner, H. (1991). Lower receptor avidity required for thymic clonal deletion than for effector T-cell function. *Nature,* **351**, 482-485.

Reid, S. W., McAdam, S., Smith, K. J., Klenerman, P., O'Callaghan, C. A., Harlos, K., Jakobsen, B. K., McMichael, A. J., Bell, J. I., Stuart, D. I. & Jones, E. Y. (1996). Antagonist HIV-1 Gag peptides induce structural changes in HLA B8. *J. Exp. Med.* **184**, 2279-2286.

Reinherz, E. L., Tan, K., Tang, L., Kern, P., Liu, J., Xiong, Y., Hussey, R. E., Smolyar, A., Hare, B., Zhang, R., Joachimiak, A., Chang, H. C., Wagner, G. & Wang, J. (1999). The crystal structure of a T-cell receptor in complex with peptide and MHC class II. *Science,* **286**, 1913-1921.

Saper, M. A., Bjorkman, P. J. & Wiley, D. C. (1991). Refined structure of the human histocompatibility antigen HLA-A2 at 2.6 Å resolution. *J. Mol. Biol.* **219**, 277-319.

Sebzda, E., Kündig, T. M., Thomson, C. T., Aoki, K., Mak, S. Y., Mayer, J. P., Zamborelli, T., Nathenson, S. G. & Ohashi, P. S. (1996). Mature T-cell reactivity altered by peptide agonist that induces positive selection. *J. Exp. Med.* **183**, 1093-1104.

Sewell, A. K., Harcourt, G. C., Goulder, P. J., Price, D. A. & Phillips, R. E. (1997). Antagonism of cytotoxic T lymphocyte-mediated lysis by natural HIV-1 altered peptide ligands requires simultaneous presentation of agonist and antagonist peptides. *Eur. J. Immunol.* **27**, 2323-2329.

Sloan-Lancaster, J. & Allen, P. M. (1996). Altered peptide ligand-induced partial T-cell activation: molecular mechanisms and role in T-cell biology. *Annu. Rev. Immunol.* **14**, 1-27.

Tissot, A. C., Pecorari, F. & Plückthun, A. (2000). Characterizing the functionality of recombinant T-cell receptors *in vitro*: a pMHC tetramer based approach. *J. Immunol. Methods,* **236**, 147-165.

Valitutti, S., Müller, S., Cella, M., Padovan, E. & Lanzavecchia, A. (1995). Serial triggering of many T-cell receptors by a few peptide-MHC complexes. *Nature,* **375**, 148-151.

Valitutti, S., Müller, S., Dessing, M. & Lanzavecchia, A. (1996). Different responses are elicited in cytotoxic T-lymphocytes by different levels of T-cell receptor occupancy. *J. Exp. Med.* **183**, 1917-1921.

Young, A. C., Zhang, W., Sacchettini, J. C. & Nathenson, S. G. (1994). The three-dimensional structure of $H\text{-}2D^b$ at 2.4 Å resolution: implications for antigen-determinant selection. *Cell,* **76**, 39-50.

Zhao, R., Loftus, D. J., Appella, E. & Collins, E. J. (1999). Structural evidence of T-cell xeno-reactivity in the absence of molecular mimicry. *J. Exp. Med.* **189**, 359-370.

Zinkernagel, R. M. (1996). Immunology taught by viruses. *Science,* **271**, 173-178.

Edited by I. Wilson

(Received 22 May 2000; received in revised form 31 July 2000; accepted 4 August 2000)